nature microbiology

LETTERS

DOI: 10.1038/s41564-017-0004-7

An anti-CRISPR from a virulent streptococcal phage inhibits *Streptococcus pyogenes* Cas9

Alexander P. Hynes[1], Geneviève M. Rousseau[1], Marie-Laurence Lemay[1], Philippe Horvath[2], Dennis A. Romero[3], Christophe Fremaux[2] and Sylvain Moineau[1,4*]

The CRISPR–Cas system owes its utility as a genome-editing tool to its origin as a prokaryotic immune system. The first demonstration of its activity against bacterial viruses (phages) is also the first record of phages evading that immunity[1]. This evasion can be due to point mutations[1], large-scale deletions[2], DNA modifications[3], or phage-encoded proteins that interfere with the CRISPR–Cas system, known as anti-CRISPRs (Acrs)[4]. The latter are of biotechnological interest, as Acrs can serve as off switches for CRISPR-based genome editing[5]. Every Acr characterized to date originated from temperate phages, genomic islands, or prophages[4–8], and shared properties with the first Acr discovered. Here, with a phage-oriented approach, we have identified an unrelated Acr in a virulent phage of *Streptococcus thermophilus*. In challenging a *S. thermophilus* strain CRISPR-immunized against a set of virulent phages, we found one that evaded the CRISPR-encoded immunity >40,000× more often than the others. Through systematic cloning of its genes, we identified an Acr solely responsible for the abolished immunity. We extended our findings by demonstrating activity in another *S. thermophilus* strain, against unrelated phages, and in another bacterial genus immunized using the heterologous SpCas9 system favoured for genome editing. This Acr completely abolishes SpCas9-mediated immunity in our assays.

Bacteriophage–host dynamics are a clear example of an evolutionary arms race[9,10], with each bacterial defence mechanism (for example, restriction enzymes) countered in turn by a phage mechanism, such as phage T4's heavily modified DNA[9]. A pronounced biotechnological interest has arisen in finding proteins specifically inhibiting bacterial CRISPR–Cas immune systems, which could then serve to modulate the activity of the genome-editing tool Cas9 in vivo and limit off-target activity. However, given the relative ease of bypassing the CRISPR–Cas system (a single point mutation in a targeted region is sufficient[1]), it was not clear whether such a system would even exist.

This doubt was laid to rest with the discovery of five anti-CRISPR (Acr) genes in *Pseudomonas* temperate phages, with activity against the type I-F system[4]. Type I systems are distantly related to type II systems[11,12], such as the type II-A system of *Streptococcus pyogenes* (source of the genome-editing tool SpCas9)[13]. Although these Acrs share little homology with known sequences, bioinformatic searches in similar gene neighbourhoods assisted by an association with helix-turn-helix (HTH) motifs enabled the discovery of Acrs with activity against type I-E[6], both type I-E and type I-F[7] and subsequently against type II-C systems[8]. Most recently, HTH-associated Acrs were identified in prophages of *Listeria* strains, whose native type II-A systems appeared to target their own genome[5]. In the case of two of these, activity against SpCas9 was demonstrated. Some Acr proteins have been characterized[14–16], and their modes of action are varied[16,17]. Activities range from preventing the formation of the cleavage complex (AcrF3), interacting with the target recognition domain (Steric = AcrF1, AcrIIA2 and AcrIIA4; Allosteric = AcrF2), or occluding the cleavage site itself (AcrIIA4).

We sought to discover new Acrs by returning to a phage-first method: screening phages for their ability to bypass the immunity granted by a CRISPR–Cas system. *Streptococcus thermophilus* is a model for acquisition of new CRISPR immunities[1,2,18–21], shares its genus with the source of SpCas9, and its active CRISPR–Cas systems are also of type II-A. By challenging *S. thermophilus* strains sensitive to multiple phages, we hoped to identify phages that were less likely to lead to the acquisition of new spacers (phage-derived sequences in the CRISPR array conferring immunity). Industrial *S. thermophilus* strains are routinely challenged with virulent phages to naturally generate phage-resistant variants. The availability of a collection of hundreds of *S. thermophilus* virulent phages infecting industrial strains led to the observation that some phages generate differing proportions of CRISPR-immunized survivors. One set of five virulent phages infecting *S. thermophilus* strain DGCC7854 proved ideal, because they are easy to manipulate, the host contains a single active type II-A CRISPR–Cas system and the variability in CRISPR immunization between phages was pronounced. Two of these five phages readily gave rise to CRISPR-immune colonies, and three did not (Fig. 1, top). The dearth of spacer acquisition from these three phages did not necessarily confirm the presence of Acrs. Those phages could simply be more sensitive to non-CRISPR forms of resistance, be quicker to take over the host cell, or produce fewer immunogenic defective particles[18]. Thus, it was necessary to establish whether the CRISPR–Cas system was impeded during the adaptation ('memorization' of new targets though spacer acquisition) or interference (cleavage of that target) process. Using plasmid programming[19], we generated a CRISPR-immunized strain containing a new spacer targeting a sequence conserved in all five phage genomes. Then, in plaquing each phage upon this strain, we observed that four of the five phages suffered a drastic (~4–6 $\log_{10}$) reduction in titre consistent with CRISPR interference, but one phage, D4276, did not (Fig. 1, bottom). The resulting plaques ($n = 10$), when purified upon the immune strain, contained the wild-type protospacer target sequence. We categorized our phages

[1]Département de biochimie, de microbiologie, et de bioinformatique, Faculté des sciences et de génie, Groupe de recherche en écologie buccale, Faculté de médecine dentaire, Université Laval, Québec City, QC G1V 0A6, Canada. [2]DuPont Nutrition and Health, BP 10, 86220 Dangé-Saint-Romain, France. [3]DuPont Nutrition and Health, 3329 Agriculture Dr, Madison, WI 53716, USA. [4]Félix d'Hérelle Reference Center for Bacterial Viruses, Faculté de médecine dentaire, Université Laval, Québec City, QC G1V 0A6, Canada. *e-mail: Sylvain.Moineau@bcm.ulaval.ca

© 2017 Macmillan Publishers Limited, part of Springer Nature. All rights reserved.

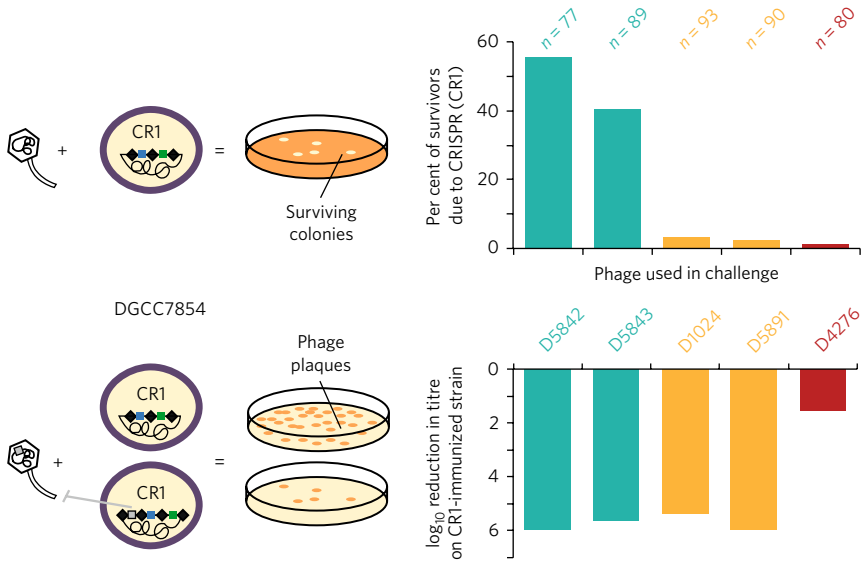


Fig. 1 | Discovery of virulent phages impeding CRISPR-based immunity. Top: when a virulent phage is used to challenge a bacterium, phage-resistant survivors can be isolated. When *S. thermophilus* DGCC7854 colonies ($n = 77$–93) surviving infection by one of five virulent phages were screened, the frequencies of CRISPR-immune survivors differed by phage. Bottom: when comparing these same phages plated on the phage-sensitive wild-type strain DGCC7854 and a CRISPR-immunized derivative targeting a sequence conserved in all five phages, a large reduction in phage titre was observed. Phage D4276 exhibited a much smaller reduction in titre than the other four related phages. Phage names and associated data are coloured according to CRISPR-interacting phenotype: sensitive (green), impeded adaptation (ochre) and resistant (red).

according to these CRISPR-interacting phenotypes: green for CRISPR-sensitive (allows both adaptation and interference) phages D5842 and D5843, ochre for impeded adaptation (still susceptible to immunity, once acquired) phages D1024 and D5891, and red for the CRISPR-resistant (bypassing the immunity conferred by a targeting spacer) phage D4276, a candidate to harbour an Acr. We believe these assays can be used to rapidly screen phages of adaptation-competent strains for other Acrs.

We set about systematically cloning genes from the resistant phage D4276 (GenBank MF161328) into a high-copy plasmid where they could be expressed in the CRISPR-immunized strain (Fig. 2a). A phage gene encoding an Acr should inactivate the pre-existing CRISPR-immunity and thereby restore the titre of a sensitive phage plated upon the strain. In this manner, we found one gene, *acrIIA5* (locus D4276_028), which completely restored the immunized strain's sensitivity to the sensitive phage D5842 (~6 $\log_{10}$ increase), as well as increased sensitivity to the resistant phage D4276, back to wild-type levels (Fig. 2b). We attribute this increase in phage titre for even the Acr-containing phage D4276 to high Acr production before phage exposure, which would otherwise be a time-sensitive process whereby production must outrace CRISPR–Cas activity. To ensure that the gain-of-sensitivity phenotypes were due only to the Acr, we allowed loss of the Acr-bearing plasmid and confirmed a return of resistance by spot tests, where it was indistinguishable from the parent strain ($P > 0.8$).

As all five phages infecting DGCC7854 are related *cos*-type phages, we could not rule out that the Acr might be dependent upon interaction with other proteins present in these phages. Furthermore, strain DGCC7854 contains a single active CRISPR–Cas system (CRISPR1; CR1), as opposed to two systems (CR1 and CRISPR3; CR3) often active in *S. thermophilus* strains. We ported our Acr vector over to the well-characterized model strain, *S. thermophilus* DGCC7710, which is sensitive to an unrelated virulent *pac*-type phage 2972, and for which we have strains immunized at either the CR1 (with a Cas9 sharing 99% amino acid identity with that of *S. thermophilus* DGCC7854, over 100% of the protein length) or CR3 locus (Fig. 2c) (with a Cas9 sharing 23% amino acid identity with DGCC7854, over 63% of the protein length). In *S. thermophilus* DGCC7710, the Acr activity was maintained, completely restoring phage sensitivity to a CR1-immunized strain and partially restoring sensitivity to a CR3-immunized strain. When we attempted immunization assays with the CRISPR-sensitive virulent phage 2972 on DGCC7710 bearing the Acr, the number of surviving colonies fell sharply (Fig. 2d). Moreover, the nature of those survivors changed drastically. The number of CR3-immune colonies dropped, a number of previously undetectable non-CRISPR mutants were observed and, whereas CR1 immunizations normally comprise upwards of 90% of surviving colonies[22], only a single colony with a CR1 spacer acquisition was recovered (Fig. 2d). Of note, the CR1 spacer in question targeted the plasmid (still present and carrying an intact *acrIIA5*), rather than the phage genome. It is possible that AcrIIA5 impedes Cas9-mediated cleavage, but not the role of Cas9 in spacer acquisition[23].

The AcrIIA5 protein is homologous to a number of uncharacterized proteins of phage or streptococcal origin (Fig. 3a). So far, all confirmed Acrs originate from temperate phages, prophage regions, or genomic islands[4–8], although two (more distant) Acr homologues have been detected in virulent phage genomes[5]. These previously identified Acrs have either had, or been genetically adjacent to proteins having, a characteristic HTH motif. Although no such nearby motif was detected for AcrIIA5 in the virulent streptococcal phage, its homologues in temperate phages are upstream of a conserved protein with a predicted HTH motif. In phage genomes, homologues of *acrIIA5* appear to be in the highly variable region downstream of the holin-endolysin gene cassette involved in cell lysis (Fig. 3a). In streptococcal genomes, the homologues are not in characteristic genomic islands. Protein AcrIIA5 is 140 amino acids long (Fig. 3b), and other previously discovered Acrs range from 50 to 150 amino acids in length[5]. The protein sequence is predicted to contain a distinctive coiled-coil motif, which might act in a nucleic acid binding role, similar to HTH and AP2 motifs associated with other Acrs[5].

Although the genome-editing tool SpCas9 is more closely related to the Cas9 of the CR3 system of *S. thermophilus* (58% amino

© 2017 Macmillan Publishers Limited, part of Springer Nature. All rights reserved.

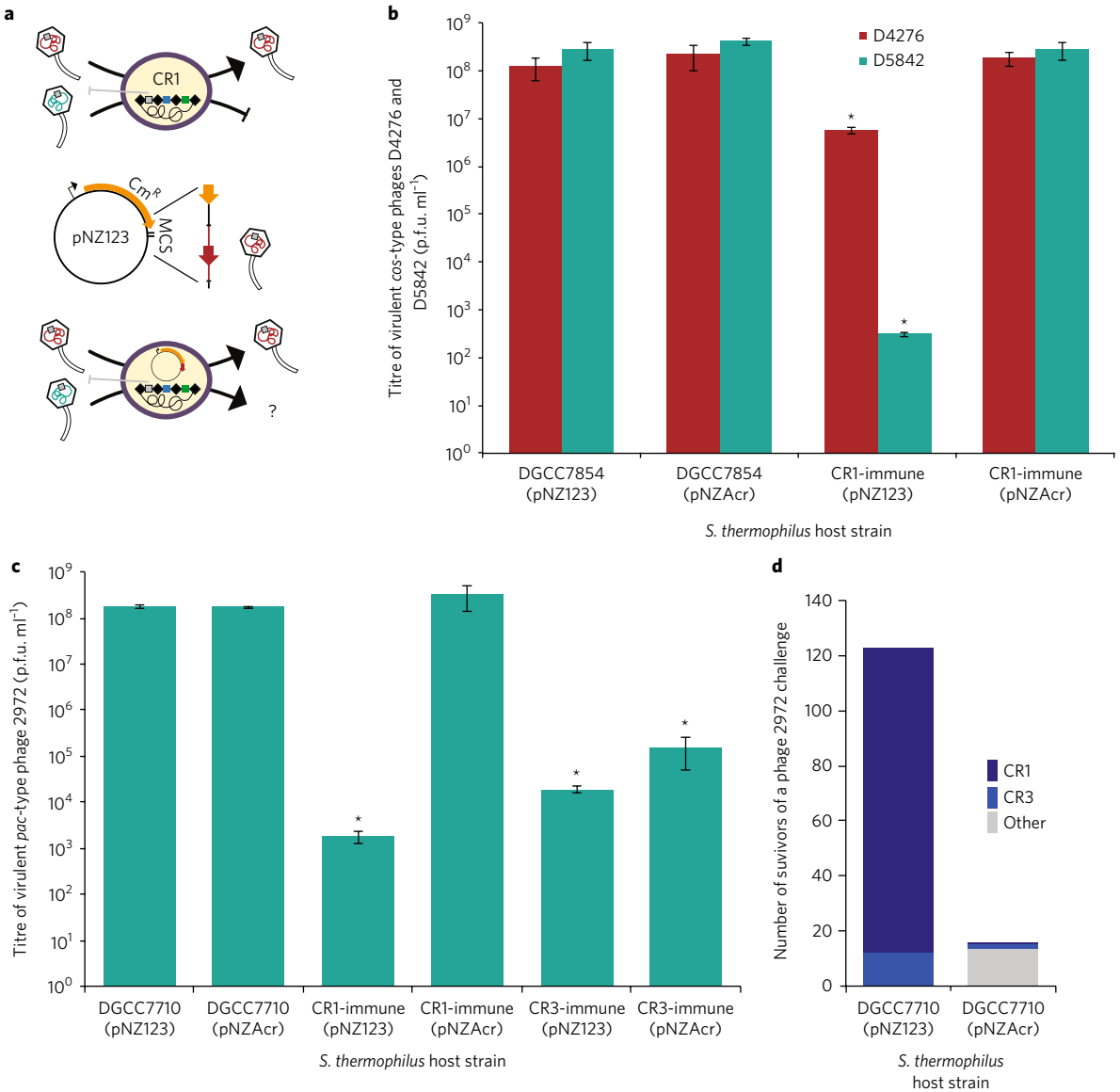
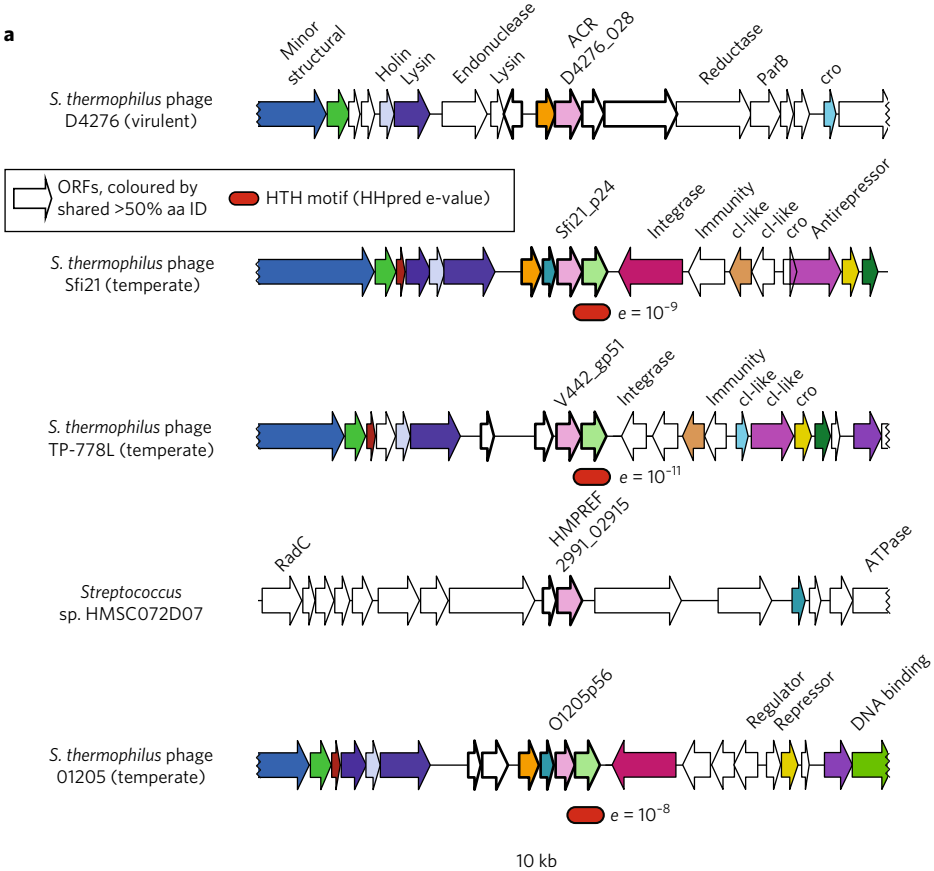


Fig. 2 | Anti-CRISPR activity of AcrIIA5 in *S. thermophilus*. **a**, Genes cloned from the CRISPR-resistant (red) phage D4276 were expressed in the *S. thermophilus* DGCC7854-derived CRISPR-immunized strain, and the resulting transformants were assayed for increased sensitivity to the sensitive (green) phage D5842. MCS, multiple cloning site. **b**, Titre of the resistant (red) *cos*-type phage D4276 and sensitive (green) *cos*-type phage D5842 on the naive DGCC7854 or its CR1-immune derivative, carrying either the empty vector pNZ123 or the vector expressing AcrIIA5 (pNZAcr). Each column depicts the average of three biological replicates, each of three technical replicates. **c**, Titre of the sensitive (green) *pac*-type phage 2972 on the naive *S. thermophilus* DGCC7710, a CR1-immune mutant or a CR3-immune mutant, carrying either the empty vector pNZ123 or the vector expressing AcrIIA5 (pNZAcr). Each column depicts the average of three biological replicates, each of three technical replicates. In **b** and **c**, error bars represent standard deviation. An asterisk denotes a difference ($^*P < 0.001$) from all other data, and no other strain differed from any other ($P > 0.5$); determined by one-way analysis of variance (ANOVA) and Tukey's honest significant difference (HSD) test. **d**, Number and characterization of survivors following a phage 2972 challenge of DGCC7710, carrying either the empty vector pNZ123 or the vector expressing AcrIIA5 (pNZAcr). The single CR1 acquisition detected in the presence of the Acr targeted the plasmid and not the phage. CR3 acquisitions targeted the phage, as expected. All cells maintained an intact *acrIIA5*.

acid identity over 99% of the CR3 Cas9 length in *S. thermophilus* DGCC7710) than to that of the CR1 system (25% amino acid identity over 69% of the CR1 Cas9 length in *S. thermophilus* DGCC7854), we were keen to determine whether AcrIIA5 would have any effectiveness against SpCas9. We initially attempted to assay the effectiveness of AcrIIA5 (pNZAcr) on SpCas9 (pCas9)[24] in *Escherichia coli*, but although we managed to clone each separately, the two systems were not able to coexist in *E. coli*. We suspect some aspect of the Acr–Cas9 interaction is pernicious to *E. coli*. Instead, we used a pCas9 derivative adjusted for use in *Lactococcus lactis*, with demonstrated efficacy in the genome editing of virulent phages[25] (Fig. 4a).

The pL2Cas9-44 construct, targeting *orf44* of the virulent phage p2, resulted in a 4 $\log_{10}$ decrease in phage titre (Fig. 4b), which was completely restored by the presence of the Acr provided on another plasmid. Curiously, the 4 $\log_{10}$ reduction associated with pL2Cas9-44 was also accompanied by a 'tiny plaque' phenotype that proved difficult to quantify, as it was only observable on some technical replicates. The maximum number of tiny plaques observed is displayed in pale orange in Fig. 4b. We characterized the phenotype and genotype of these smaller plaques in detail (Supplementary Fig. 1), establishing that they were CRISPR-bypassing mutants genetically indistinguishable from those in the larger plaques, but arising only

© 2017 Macmillan Publishers Limited, part of Springer Nature. All rights reserved.



b

```
                                                                    H H H H H H H H
D4276     1 MAYGKSRYNSYRKRSFNRSNKQRREYAQ 28
Sfi21
TP778-L                              I  DTK       K
Streptococcus sp.      F   N    P       D   C
01205                                   D

                  H H H H H H H H H H H H
D4276    29 EMDRLEKAFENLDGWYLSSMKDSAYKDF 56
Sfi21
TP778-L          EK   Q    K
Streptococcus sp. A  E   Q    E      H      M       N
01205                 QT   K

                  E E E E E                                  E E E E E
D4276    57 GKYEIRLSNHSADNKYHDLENGRLIVNI 84
Sfi21                                                        V
TP778-L                                                      V
Streptococcus sp. E   QV           Q          Y            V
01205                                                        V

                                  H H H H H H H H H H H H H H H
D4276    85 KASKLNFVDIIENKLDKIIEKIDKLDLD 112
Sfi21                                                  T
TP778-L
Streptococcus sp.                          L   V
01205               K   ------------------

                  E E                 H H H H H
D4276   113 KYRFINATNLEHDIKCYYKGFKTKKEVI 140
Sfi21               K   R          Y     D
TP778-L             RM                    D
Streptococcus sp.                  L   Y  D
01205   ------------                      D
```

Fig. 3 | Anti-CRISPR gene and protein. a, Genomic context of the gene encoding the Acr in all phage homologues, as well as the closest non-phage homologue (using BLASTp)[30,31]. The Acr homologue is centred, in light pink and identified by a locus tag. Gene function, where known, is annotated. Open reading frames (ORFs) are coloured if their predicted protein product shares ≥50% amino acid identity (aa ID) with another in the data set consisting of the full phage genomes, and are white if they do not. Genes with a bold outline were subjected to a search for HTH motifs by HHpred[32], and if hits matched PDB structures with known HTH motifs, the e-value of the hit is reported. **b**, Protein alignment of all phage Acr homologues, as well as the closest non-phage homologue (using BLASTp), highlighting only differences. A dash (–) indicates the residue is absent from the protein. Coloured residues are predicted coiled-coil motifs (PCOILS, >90% confidence)[32] from the consensus, while 'E' (extended) and 'H' (helical) indicators above the residue are the consensus predictions obtained from jnet, jhmm and jpssm[33].

© 2017 Macmillan Publishers Limited, part of Springer Nature. All rights reserved.

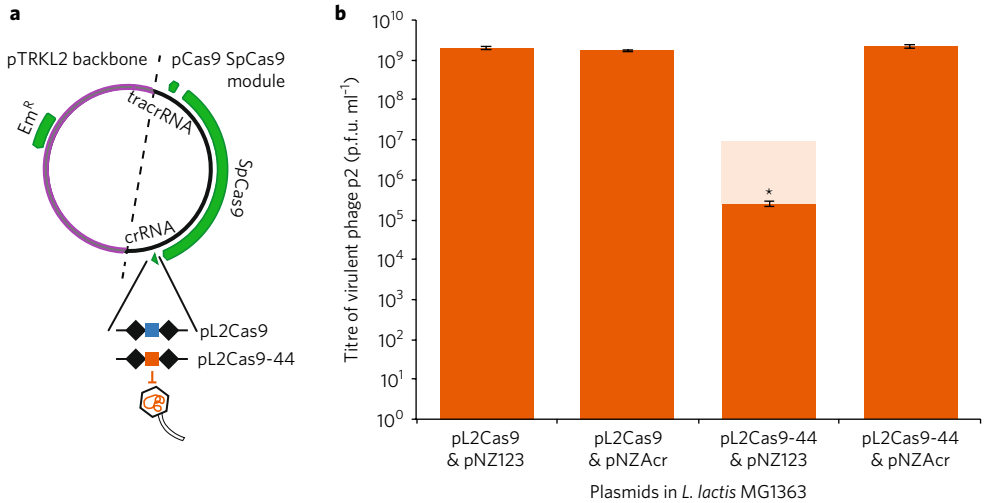


Fig. 4 | Anti-CRISPR activity against SpCas9. a, Generating an immunized *L. lactis* MG1363 strain. pL2Cas9[25] contains the SpCas9 module from pCas9[24] on a pTRKL2[34] vector backbone. A spacer targeting *orf44* of *L. lactis* virulent phage p2 was cloned to create a phage-targeting SpCas9. tracrRNA, trans-activating crRNA. **b**, Titre of virulent phage p2 on its host *L. lactis* MG1363 carrying either pL2Cas9 or pL2Cas9 targeting the phage (pL2Cas9-44) and either the empty vector pNZ123 or the vector expressing AcrIIA5 (pNZAcr). The titre was assayed by spot test and each bar represents an average of three biological replicates, each of three technical replicates. Only plaques with typical morphology were counted, although a secondary morphology of tiny phage plaques occasionally appeared when plated on pL2Cas9-44 with pNZ123. Although these plaques were not reliably countable, the maximum threshold at which they appeared is depicted by a pale orange box. Error bars represent standard deviation and an asterisk denotes a difference ($^*P < 0.001$) from all other data, while no other strain differed from any other ($P > 0.5$) as determined by one-way ANOVA and Tukey's HSD test.

after several rounds of replication on the 'leaky' (4 $\log_{10}$ reduction) targeting strain. Notably, however, the expression of the Acr completely rescued both the titre and the tiny-plaque phenotype.

AcrIIA5 is the first Acr with demonstrated activity from a virulent phage, is structurally distinct from previously characterized Acrs, and displays complete in vivo inhibition of SpCas9-mediated immunity. It seems oddly fitting that this discovery brings the field of anti-CRISPRs full circle, back to the bacterial species that first drew the world's attention to CRISPR–Cas systems[1]—*S. thermophilus*.

Methods

As *S. thermophilus* is a model for the study of CRISPR adaptation, a detailed step-by-step protocol for many of the methods used here is available elsewhere[20]. Where applicable, each section header refers explicitly to the steps in the cited protocol.

Strain culturing (Step 1 in ref. [20]). *S. thermophilus* cultures were grown in M17 medium (Oxoid) supplemented with 0.5% wt/vol lactose (LM17). Chloramphenicol (Cm), when necessary, was added at 5 μg ml^{-1}. When used to generate an overnight culture for use the following day, cultures were grown at 37 °C without shaking. In all other cases, they were grown at 42 °C without shaking. If phages were to be added, the medium was further supplemented with 10 mM $CaCl_2$.

L. lactis cultures were grown in M17 medium supplemented with 0.5% wt/vol glucose monohydrate (GM17). Chloramphenicol or erythromycin, when necessary, was also added at 5 μg ml^{-1}. Cultures were grown at 30 °C without shaking, except when the activity of an SpCas9-containing construct was assayed, in which case incubations took place at 33 °C. If phage p2 was to be added, the medium was further supplemented with 10 mM $CaCl_2$.

E. coli cultures were grown in lysogeny broth medium. Chloramphenicol, when necessary, was provided at 20 μg ml^{-1}. Cultures were grown at 37 °C with shaking.

For all strains used in this study, see Supplementary Table 1.

Phage amplification (Steps 1–12 in ref. [20]). A scraping from a phage lysate preserved at −80 °C with 15% glycerol was co-inoculated with its host strain, in medium supplemented with 10 mM $CaCl_2$ and grown until complete lysis was observed. This first amplification lysate was then filtered through a 0.45 μm polyethersulfone (PES) filter and 100 μl was used to inoculate its host strain grown to an optical density at 600 nm (OD_{600}) of 0.1 in medium supplemented with 10 mM $CaCl_2$. This second amplification lysate was also filtered through a 0.45 μm PES filter, then stored at 4 °C.

For all phages used in this study see Supplementary Table 1.

Phage titration (Steps 13–23 in ref. [20]). Spot test (Figs. 1 and 4). Phages were serially diluted in phage buffer (50 mM Tris-HCl, pH 7.5, 100 mM NaCl, 8 mM $MgSO_4$). Volumes (3 ml) of molten 0.75% agar medium at 55 °C, supplemented with 10 mM $CaCl_2$, were inoculated with 300 μl of an overnight culture of the host strain, then rapidly poured over a pre-set plate of the same medium with 1% agar. The plate was allowed to set and dry. Phage dilutions, 5 μl from each, were spotted onto the dry overlay and allowed to dry for 20 min. The plates were then incubated overnight and plaques counted at the lowest dilution at which they were visible.

Full (Fig. 2). Phages were serially diluted in phage buffer. Volumes (3 ml) of molten 0.75% agar medium at 55 °C, supplemented with 10 mM $CaCl_2$, were co-inoculated with 300 μl of an $OD_{600} = 0.6$ culture of the host strain and 100 μl of diluted phages. The plates were then incubated overnight and plaques counted from plates with between 30 and 300 plaques.

Immunizing assays (Steps 24–37 in ref. [20]). These are also referred to as 'BIM assays' (bacteriophage insensitive mutants). Phages were diluted in phage buffer to obtain a final multiplicity of infection (MOI) of 0.1 plaque-forming units per colony-forming unit (p.f.u./c.f.u.). Volumes (3 ml) of molten 0.75% agar LM17 medium at 55 °C, supplemented with 10 mM $CaCl_2$, were co-inoculated with 300 μl of a culture at an OD_{600} of 0.6 (~1.2×10^8 c.f.u. ml^{-1}) of the host strain and 100 μl of the appropriate phage dilution. The plates were then incubated overnight at 42 °C and surviving colonies were counted.

Characterization of surviving colonies (Steps 38–54 in ref. [20]). Random surviving colonies after the virulent phage challenge assay were screened by PCR for acquisition of new spacers at the CRISPR1 (CR1) and CRISPR3 (CR3) loci (DGCC7710) or CR1 locus (DGCC7854) using the primers described in Supplementary Table 1. An increase in the size of the PCR product relative to the wild-type was indicative of CRISPR immunization. The resulting PCR products were sequenced to confirm the identity of the newly acquired spacer(s). For the assays in Fig. 2, 32 phage-resistant colonies with pNZAcr were screened, as well as 20 pNZ123 colonies. Where relevant, the presence of the insert in pNZAcr was confirmed by sequencing in cells that had acquired new spacers.

Transformation (Box 3 in ref. [20]). Commercial NEB5α *E. coli* cells were transformed according to the manufacturer's recommendations (New England Biolabs). *S. thermophilus* strains were transformed by growing them to an OD_{600} of 0.4, subjecting them to a glycine shock for 1 h, repeated washes and then electroporated. *L. lactis* strains were transformed using a similar glycine-based protocol[26].

Plasmid programming (Boxes 5 and 6 in ref. [20]). A plasmid was designed to contain a protospacer (CRISPR-acquirable sequence) targeting the five phages used in the challenges. Two oligos (5phage_tmp_F and 5phage_tmp_R; see

© 2017 Macmillan Publishers Limited, part of Springer Nature. All rights reserved.

Supplementary Table 1) consisting of a conserved protospacer in the gene encoding the tape measure protein, as well as overhangs suited for cloning, were annealed together by mixing them in equal parts, heating them to 98 °C, then cooling them slowly to 50 °C. This annealed construct was then ligated directly into an EcoRI/XhoI double-digested pNZ123, transformed into commercial NEB5α, and selected for with chloramphenicol. The constructed plasmid was then isolated using Qiaprep Spin Miniprep kit (Qiagen) according to the manufacturer's recommendations. *S. thermophilus* DGCC7854 was transformed with this plasmid, pNZ5phage, then grown in the absence of selection for seven generations and subjected to an immunizing assay (see section 'Immunizing assays') with phage D5842. The surviving colonies had naturally acquired the desired spacer from the plasmid[19] in their CRISPR array, immunizing them to the phages. The spacer sequence was confirmed as described in the section 'Characterization of surviving colonies'.

For all plasmids used in this study, see Supplementary Table 1.

Phage genome sequencing and annotation. DNA from the virulent streptococcal phage D4276 was purified using a PureLink Viral RNA/DNA kit (Invitrogen). The purified DNA was sequenced on a MiSeq system using a MiSeq reagent kit v.2 after preparation using the Nextera XT DNA library preparation kit (Illumina). The resulting reads were assembled using Ray version 2.2.0[27]. The genome was annotated using ORF-FINDER[28] and GeneMark.hmm prokaryotic[29] and the annotations were manually curated based on comparisons to related phages. The complete annotated genomic sequence of phage D4276 has been deposited in GenBank under accession no. MF161328.

Phage gene cloning and pNZAcr construction. Primers were designed to systematically clone all genes of phage D4276 into pNZ123 oriented so as to drive transcription from the promoter upstream of the chloramphenicol resistance gene, *cat*. Initially, inserts were designed to contain several genes, but if cloning failed, the inserts were redesigned as smaller, single-gene constructs. The gene of greatest interest, D4276_028, exemplifies this cloning technique. Primers D4276_28_F and D4276_28_R (Supplementary Table 1) were designed to amplify the gene and append 30 nt extensions overlapping the pNZ123 cloning sites. The amplified gene was then cloned by Gibson reaction into XbaI-digested pNZ123. The resulting plasmid, pNZAcr, was transformed into commercial NEB5a, isolated using a Qiaprep Spin Miniprep kit and then transformed into the relevant *S. thermophilus* and *L. lactis* strains. The sequence of the insert was confirmed by sequencing using primers pNZins_F and pNZins_R (Supplementary Table 1).

Plasmid loss assays. *S. thermophilus* cultures carrying pNZAcr were serially grown in the absence of antibiotic selection, inoculating fresh 10 ml of LM17 broth medium with 100 µl of a culture grown to saturation. This was repeated five times. Dilutions of the resulting culture were spread on plates to obtain isolated colonies, and 120 such colonies were then patch-plated on LM17 with and without chloramphenicol. Colonies, which grew on LM17 (all 120) but failed to grow on LM17 Cm (two), were screened by PCR to confirm plasmid loss using primers pNZins_F and pNZins_R (Supplementary Table 1), and their CR1 locus was amplified to confirm the presence of the immunizing spacer. Colonies were then used to titre phages D4276 (CRISPR-resistant) and D5842 (CRISPR-sensitive) and confirm that they had regained resistance to the phages from losing the plasmid.

AcrIIA5 analysis. The protein sequence of D4276_028, its neighbours, its homologues and their neighbours were subjected to analysis through BLASTp[30,31], HHpred[32], PCOILS[32] and jPred4[33].

pL2Cas9-44 construction. pL2Cas9[25] is a derivative of the lactococcal vector pTRKL2[34] with the SpCas9 module of pCas9[24]. A pair of primers consisting of a spacer sequence targeting *orf44* of phage p2 and overhangs for ligation into pL2cas9 were designed (PS_44 and PS_44_RC). They were annealed together by mixing them in equal parts, heating them to 98 °C, then cooling them slowly to 50 °C. This annealed construct was then ligated into digested pL2Cas9 and transformed directly into *L. lactis*. The resulting transformants were screened by PCR amplification and sequencing to confirm the presence of the desired spacer, using primers Cas9_S.pyo_F6 and crRNA_S.pyo_R (Supplementary Table 1).

Efficiency of centres of infection. Cultures of all four *L. lactis* strains depicted in Fig. 4b were grown at 33 °C to an OD_{600} of 0.8 (~1.9×10^8 c.f.u. ml^{-1}), concentrated twofold by pelleting and resuspending in a half-volume of fresh GM17 medium with 10 mM $CaCl_2$. Phage p2 was then added to an MOI of 0.2, mixed by inversion and given 5 min to allow adsorption to the cells at 33 °C. The phage–cell mix was next spun down and resuspended in fresh medium three times to wash away unbound phages, and serially diluted. Then, 100 µl of the resulting dilutions were added to 300 µl of indicator strain (*L. lactis* MG1363 pNZ123 pL2Cas9), embedded in a soft agar overlay (see section 'Phage titration'), and incubated at 33 °C overnight.

Investigating the tiny-plaque phenotype. Plaques were obtained from phage titres on *L. lactis* MG1363 (pNZ123 pL2Cas9-44), as well as efficiencies of centres of infection assays where phage p2 was passaged on MG1363 (pNZ123 pL2Cas9-44) but plated on the sensitive indicator. Ten plaques from each condition were lifted from those plates using a wide-mouth micropipette tip and resuspended in phage buffer. This mix was used as a template for PCR, using primers CB13.10 and CB14.6, to assess the sequence of the targeted region in the phage (*orf44*). Each mix was also plated anew on strain *L. lactis* MG1363 pNZ123 pL2Cas9-44 and the morphology of the resulting plaques was characterized.

Data availability. The data that support the findings of this study are available from the corresponding author upon request.

Received: 25 May 2017; Accepted: 4 July 2017;
Published online: 07 August 2017

References

1. Barrangou, R. et al. CRISPR provides acquired resistance against viruses in prokaryotes. *Science* **315**, 1709–1712 (2007).
2. Deveau, H. et al. Phage response to CRISPR-encoded resistance in *Streptococcus thermophilus*. *J. Bacteriol.* **190**, 1390–1400 (2008).
3. Bryson, A. L. et al. Covalent modification of bacteriophage T4 DNA inhibits CRISPR–Cas9. *mBio* **6**, e00648-15 (2015).
4. Bondy-Denomy, J., Pawluk, A., Maxwell, K. L. & Davidson, A. R. Bacteriophage genes that inactivate the CRISPR/Cas bacterial immune system. *Nature* **493**, 429–432 (2013).
5. Rauch, B. J. et al. Inhibition of CRISPR–Cas9 with bacteriophage proteins. *Cell* **168**, 150–158 (2017).
6. Pawluk, A., Bondy-Denomy, J., Cheung, V. H. W., Maxwell, K. L. & Davidson, A. R. A new group of phage anti-CRISPR genes inhibits the type I-E CRISPR–Cas system of *Pseudomonas aeruginosa*. *mBio* **5**, e00896-14 (2014).
7. Pawluk, A. et al. Inactivation of CRISPR–Cas systems by anti-CRISPR proteins in diverse bacterial species. *Nat. Microbiol.* **1**, 16085 (2016).
8. Pawluk, A. et al. Naturally occurring off-switches for CRISPR–Cas9. *Cell* **167**, 1829–1838 (2016).
9. Labrie, S. J., Samson, J. E. & Moineau, S. Bacteriophage resistance mechanisms. *Nat. Rev. Microbiol.* **8**, 317–327 (2010).
10. Samson, J. E., Magadán, A. H., Sabri, M. & Moineau, S. Revenge of the phages: defeating bacterial defences. *Nat. Rev. Microbiol.* **11**, 675–687 (2013).
11. Makarova, K. S. et al. An updated evolutionary classification of CRISPR–Cas systems. *Nat. Rev. Microbiol.* **13**, 722–736 (2015).
12. Makarova, K. S., Zhang, F. & Koonin, E. V. SnapShot: class 2 CRISPR–Cas systems. *Cell* **168**, 328–328 (2017).
13. Jinek, M. et al. A programmable dual-RNA-guided DNA endonuclease in adaptive bacterial immunity. *Science* **337**, 816–821 (2012).
14. Chowdhury, S. et al. Structure reveals mechanisms of viral suppressors that intercept a CRISPR RNA-guided surveillance complex. *Cell* **169**, 47–57 (2017).
15. Maxwell, K. L. et al. The solution structure of an anti-CRISPR protein. *Nat. Commun.* **7**, 13134 (2016).
16. Dong, D. et al. Structural basis of CRISPR–SpyCas9 inhibition by an anti-CRISPR protein. *Nature* **546**, 436–439 (2017).
17. Bondy-Denomy, J. et al. Multiple mechanisms for CRISPR–Cas inhibition by anti-CRISPR proteins. *Nature* **526**, 136–139 (2015).
18. Hynes, A. P., Villion, M. & Moineau, S. Adaptation in bacterial CRISPR–Cas immunity can be driven by defective phages. *Nat. Commun.* **5**, 4399 (2014).
19. Hynes, A. P., Labrie, S. J. & Moineau, S. Programming native CRISPR arrays for the generation of targeted immunity. *mBio* **7**, e00202-16 (2016).
20. Hynes, A. P. et al. Detecting natural adaptation of the *Streptococcus thermophilus* CRISPR–Cas systems in research and classroom settings. *Nat. Protoc.* **12**, 547–565 (2017).
21. Wei, Y., Chesne, M. T., Terns, R. M. & Terns, M. P. Sequences spanning the leader-repeat junction mediate CRISPR adaptation to phage in *Streptococcus thermophilus*. *Nucleic Acids Res.* **43**, 1749–1758 (2015).
22. Magadán, A. H., Dupuis, M.-È., Villion, M. & Moineau, S. Cleavage of phage DNA by the *Streptococcus thermophilus* CRISPR3-Cas system. *PLoS ONE* **7**, e40913 (2012).
23. Heler, R. et al. Cas9 specifies functional viral targets during CRISPR–Cas adaptation. *Nature* **519**, 199–202 (2015).
24. Jiang, W., Bikard, D., Cox, D., Zhang, F. & Marraffini, L. A. RNA-guided editing of bacterial genomes using CRISPR–Cas systems. *Nat. Biotechnol.* **31**, 233–239 (2013).
25. Lemay, M.-L., Tremblay, D. M. & Moineau, S. Genome engineering of virulent lactococcal phages using CRISPR–Cas9. *ACS Synth. Biol.* **6**, 1351–1358 (2017).
26. Holo, H. & Nes, I. F. High-frequency transformation, by electroporation, of *Lactococcus lactis* subsp. cremoris grown with glycine in osmotically stabilized media. *Appl. Env. Microbiol.* **55**, 3119–3123 (1989).

© 2017 Macmillan Publishers Limited, part of Springer Nature. All rights reserved.

27. Boisvert, S., Raymond, F., Godzaridis, E., Laviolette, F. & Corbeil, J. Ray Meta: scalable de novo metagenome assembly and profiling. *Genome Biol.* **13**, R122 (2012).
28. Rombel, I. T., Sykes, K. F., Rayner, S. & Johnston, S. A. ORF-FINDER: a vector for high-throughput gene identification. *Gene* **282**, 33–41 (2002).
29. Lukashin, A. V. & Borodovsky, M. GeneMark.hmm: new solutions for gene finding. *Nucleic Acids Res.* **26**, 1107–1115 (1998).
30. Altschul, S. F., Gish, W., Miller, W., Myers, E. W. & Lipman, D. J. Basic local alignment search tool. *J. Mol. Biol.* **215**, 403–410 (1990).
31. Altschul, S. F. et al. Gapped BLAST and PSI-BLAST: a new generation of protein database search programs. *Nucleic Acids Res.* **25**, 3389–3402 (1997).
32. Alva, V., Nam, S.-Z., Söding, J. & Lupas, A. N. The MPI bioinformatics Toolkit as an integrative platform for advanced protein sequence and structure analysis. *Nucleic Acids Res* **44**, W410–W415 (2016).
33. Drozdetskiy, A., Cole, C., Procter, J. & Barton, G. J. JPred4: a protein secondary structure prediction server. *Nucleic Acids Res.* **43**, W389–W394 (2015).
34. O'Sullivan, D. J. & Klaenhammer, T. R. High- and low-copy-number *Lactococcus* shuttle cloning vectors with features for clone screening. *Gene* **137**, 227–231 (1993).

Acknowledgements

The authors thank M.-C. Jodeau and I. Chavichvily for the initial technical work on the efficiency of spacer acquisition in *S. thermophilus* DGCC7854. A.P.H. is supported by an NSERC Postdoctoral Fellowships award. M.-L.L. is supported by scholarships from the Fonds de Recherche du Québec-Nature et Technologies, Novalait and Op+Lait. S.M. acknowledges funding from the Natural Sciences and Engineering Research Council of Canada (NSERC) Discovery Program and DuPont. S.M. holds a Tier 1 Canada Research Chair in Bacteriophages.

Author contributions

A.P.H. and S.M. jointly conceived the study. G.M.R., M.-L.L., P.H., D.A.R., and C.F. contributed technical guidance. A.P.H. designed all experiments performed in this study. A.P.H. and G.M.R. generated all subsequent data presented in the manuscript. M.-L.L. created plasmid constructs for the experiments presented in Fig. 4. A.P.H. wrote the manuscript. A.P.H. generated all associated figures. G.M.R., M.-L.L., P.H., D.A.R., C.F. and S.M commented on the manuscript.

Competing interests

A.P.H., G.M.R., M.-L.L., P.H., D.A.R., C.F. and S.M. are co-inventors on patent(s) or patent application(s) related to CRISPR–Cas systems and their various uses.

Additional information

Supplementary information is available for this paper at doi:10.1038/s41564-017-0004-7.

Reprints and permissions information is available at www.nature.com/reprints.

Correspondence and requests for materials should be addressed to S.M.

Publisher's note: Springer Nature remains neutral with regard to jurisdictional claims in published maps and institutional affiliations.

© 2017 Macmillan Publishers Limited, part of Springer Nature. All rights reserved.